

Electrical Conductivity of Tungsten in a Continuous Transition from Condensed to Gaseous State¹

A. D. Rakhel,^{2,3} V. N. Korobenko,² A. I. Savvatimski,² and V. E. Fortov²

A pulse heating technique is developed that makes it possible to investigate the transition of a metal from a condensed to a gaseous state while maintaining almost uniform temperature and pressure distributions in a sample. By means of the technique, the electrical conductivity of tungsten was measured in a process during which a pressure in the range of 30–100 kbar was applied to the sample and its density decreased from the standard solid density to a density 15–20 times less. Since the pressures are substantially higher than the critical pressure, the transition from a condensed to a gaseous state was continuous. Earlier results have shown that along isobars in the range of 30–60 kbar the density dependence of the electrical conductivity changes radically at a certain density value (at which it has a pronounced knee). At the knee, the density is approximately 10 times less than the standard solid density, and the internal energy is about two times the sublimation energy. The dependence of the electrical conductivity near the knee becomes smoother as the pressure increases. In this paper new results on the conductivity of tungsten at the pressures up to 100 kbar are presented. It is shown that the knee becomes remarkably flatter and smoother than the corresponding low pressure dependence. Nevertheless, the main features of the electrical conductivity dependence observed at low pressures persist at the maximum applied pressure.

KEY WORDS: electrical conductivity; exploding wires; liquid metal; mercury; metal–nonmetal transition; strongly coupled plasma; tungsten.

1. INTRODUCTION

The problem of transitions of metals from a condensed to a gaseous state was reported in the well-known paper by Zel'dovich and Landau [1].

¹Paper presented at the Fifteenth Symposium on Thermophysical Properties, June 22–27, 2003, Boulder, Colorado, U. S. A.

²Institute for High Energy Densities, Izhorskaya 13/19, Moscow 125412, Russia.

³To whom correspondence should be addressed. E-mail: savlab@iht.mpei.ac.ru

They noted that there is no qualitative difference between metallic and dielectric states at finite temperatures, and therefore, a transition from one state to another may be continuous. The question then arises as to the character of the phase diagrams of metals in the region where the metal-to-dielectric transition takes place. The authors predicted that, in general, metals should undergo two separate first-order phase transitions, specifically, liquid-to-vapor and metal-to-dielectric transitions with two different critical points. This question in the case of refractory metals remains unanswered because of the difficulties in performing precise measurements at high pressures and temperatures.

In a number of studies, attempts were made to measure the electrical conductivity of metals over a wide density range. Some modifications of the exploding wire technique were used [2–4] to measure the electrical conductivity of the strongly coupled metallic plasmas. The electric conductivity was determined assuming that the temperature, pressure, and other quantities are uniformly distributed over the column formed by an exploding wire (or a rolled foil [4]). At the initial stage of the heating process during which the wire evaporates, the sample was substantially non-uniform. It is assumed by the authors that the nonuniformities disappear in the later stages of the process. No direct evidence of such behavior is provided in the referenced studies.

Thus, our main motivation was to study the exploding wire dynamics when a sample (a wire or a foil), placed in a condensed dielectric medium (water, glass capillary, plastic coatings), is heated by an intense electrical current pulse. In this study a one-dimensional magneto-hydrodynamic (MHD) model was developed describing the hydrodynamic processes, which take place within a metal undergoing melting, evaporation, and ionization. The computational study has revealed the influence of different factors on the spatial distributions of physical quantities in the sample subjected to the pulse heating. Based on this study, a unique technique [5] was proposed to realize the transition of a metallic sample from a condensed to a gaseous state while maintaining the uniform distributions of the temperature and pressure in the sample.

In Ref. 6 we reported the results of experiments utilizing this technique to measure the electrical conductivity of tungsten in a process during which the pressure in the sample was maintained at a level of 30–60 kbar and the density decreased from the normal solid density to a density 15–20 times less.⁴ Since such pressures are several times higher than the critical pressure for the liquid-to-vapor phase transition (the critical

⁴In Ref. 6, as well in this study, the pressure is not a measured quantity. It is derived from one-dimensional (1D) MHD simulations of the heating dynamics.

pressure of tungsten is within 11–13 kbar [7]), evaporation did not manifest itself in these experiments. Therefore, the transition from a condensed to a gaseous state was continuous in these experiments. The point is that the volume evaporation (boiling) inevitably leads to the formation of non-uniform temperature and density distributions in the sample [7].

The experimental results presented in Ref. 6 show that, along the isobars $p = 30\text{--}35$ kbar, the density dependence of the electrical conductivity of tungsten changes radically at a certain density value, at which it has a pronounced knee.⁵ At the knee, the density is approximately ten times lower than the standard solid state density, and the internal energy is about two times the sublimation energy. For the $p = 60\text{--}65$ kbar isobars, the density dependence of the electrical conductivity near the knee becomes smoother. In this paper we present results on the electrical conductivity of tungsten obtained at pressures up to 100 kbar. It is shown that at the maximum pressure, the knee becomes flatter. The results are compared with literature data.

2. DESCRIPTION OF THE PULSE HEATING TECHNIQUE

The experiments were carried out with tungsten foil strips, with a thickness of $20\text{--}22\ \mu\text{m}$, a width of $1.5\text{--}3.0$ mm, and a length of about 1.0 cm. A foil sample was placed between two polished sapphire (or glass) plates having a thickness of $5\text{--}7$ mm, a width of 10 mm, and a length of $10.0\text{--}11.5$ mm. The side slits were filled by two mica plates (see Fig. 1). The experimental assembly was made such that the gaps between the sample and the plates were minimal. Due to the roughness of the surfaces, the gap was usually within $5\text{--}7\ \mu\text{m}$. The pulse heating of the sample was accomplished by discharging a $72\ \mu\text{F}$ capacitor bank at a charging voltage of about 18 kV.

The temporal dependences of the current through the sample and the voltage drop across its length were measured. The resistance of the sample and the Joule heat dissipated in it were determined from these two measured quantities. The electric conductivity was calculated according to the formula,

$$\sigma = \frac{l}{SR}, \quad (1)$$

where l is the sample length, R is its resistance, and S is its cross-sectional area, i.e., the product of the sample width h and thickness $d(t)$. The

⁵Prof. A. W. DeSilva has proposed to use the word “knee” to characterize the effect.

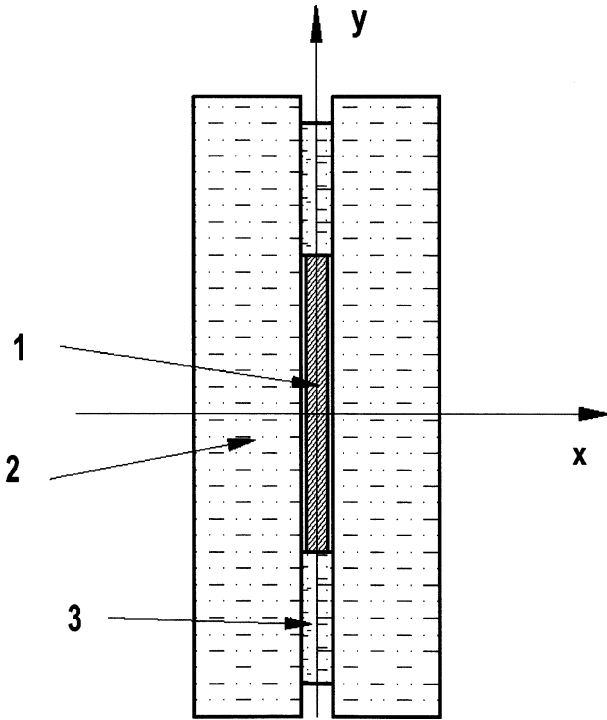


Fig. 1. Transverse cross section of experimental assembly: foil strip (1); glass plate (2); mica plate (3). The current flows in a direction perpendicular to the plane of the figure.

thickness as a function of time was calculated using a hydrodynamic model and assuming that the length and width are constant.

Basing on the numerical modeling results in the framework of the 1D MHD model [6, 7], the basic parameters of the experiments presented here were chosen so that the sample remains homogeneous during the pulse heating process. Calculations of the sample thickness in the case of homogeneous heating can be essentially simplified in comparison to those using the complete MHD model. In particular, the calculations can be performed for the prescribed temporal dependences of the Joule heat released and the electrical current through the sample (which can be taken from the corresponding experiment). In doing so, one should solve, instead of the complete system of the MHD equations, only the hydrodynamic equations (laws of conservation of mass, linear momentum, and energy), the right-hand side parts of which are some given functions of time (see Ref. 6 for detail).

Thus, the electrical conductivity is obtained using an equation of state model. The quality of the equation of state utilized in the paper was carefully analyzed [7] for the region of the liquid-to-vapor phase transition (up to the critical point). Ionization effects were described by the average atom approximation [8]. The corresponding terms were added to the thermodynamic functions used in Ref. 7. It should be noted that the average atom approximation can not reproduce accurately the ionization states in the metal–nonmetal transition region, and the corresponding uncertainties can be remarkable. We believe that our hydrodynamic calculations of the sample thickness are not essentially effected by these uncertainties as the material passes this region for a sufficiently short time.

Several experiments were performed to show that the sample remains homogeneous. In particular, experiments with different sample widths were carried out. Every experiment was repeated at least two times to get the information about the reproducibility and uncertainty of the measured quantities. These experiments have shown that current and voltage are measured with an uncertainty of less than 5%. The resistance as a function of the Joule heat released for different experiments with all parameters kept constant shows a scatter of less than 10%. To demonstrate that the complete procedure used for determination of the electrical conductivity (when some quantities are measured and other should be calculated) is self-consistent, a separate investigation was carried out. Several experiments were performed in which a thermodynamic state in the p – T plane was achieved by substantially different ways. As was shown in Ref. 6, the values of the resistivity at this state were within the experimental uncertainty of 10%.

Nevertheless, a systematic error may exist in such a procedure when the current and voltage drop are only measured and the other quantities, including the sample thickness and pressure, are calculated. To estimate the value of the possible systematic error, several experiments with mercury were performed.

3. COMPARISON WITH STEADY-STATE DATA

Results on the mercury electrical conductivity were obtained by means of the pulse heating technique presented in this paper. The main reason to investigate mercury was to compare our results with literature steady-state data in the metal-to-dielectric transition domain. For the case of mercury this domain is located at low enough temperatures and pressures and therefore, there are reliable literature data on the equation-of-state information and also the electrical conductivity. Thermodynamic information along with the critical point parameters were used to

fit the adjustable parameters of the equation-of-state model. The fitting procedure is described in Ref. 7. After fitting, the equation of state was able to reproduce reliable literature data on the critical-point parameters, the thermal expansion coefficient, and the isobaric specific heat to within 3–5%.

In the experiments on mercury, samples with a thickness of $60\ \mu\text{m}$, a width of about 3 mm, and a length of 10 mm were used. A cavity formed by two polished glass plates (having a thickness of 5 mm and a width and length of 10 mm), and two thin mica plates was filled with liquid mercury. Pulse heating of the sample was accomplished by discharging the capacitor bank at a charging voltage of about 10 kV.

The temporal dependences of the measured and some calculated quantities for mercury are presented in Fig. 2. The ratio of the resistivity to its value at standard conditions (ρ/ρ_0) versus temperature is presented in Fig. 3. As one can see our measurements are in good agreement with the steady-state data [9]. This result gives confidence that the technique used here is able to obtain reliable data on the electrical conductivity in the metal-to-dielectric transition domain.

In conclusion of this section, it should be noted that our technique has allowed us to measure the electrical conductivity of mercury over a wider temperature and density range than it was performed in Ref. 9. In our experiments the pressure increased up to 7 kbar which substantially exceeds the maximum pressure in the steady-state experiments (5 kbar) [9].

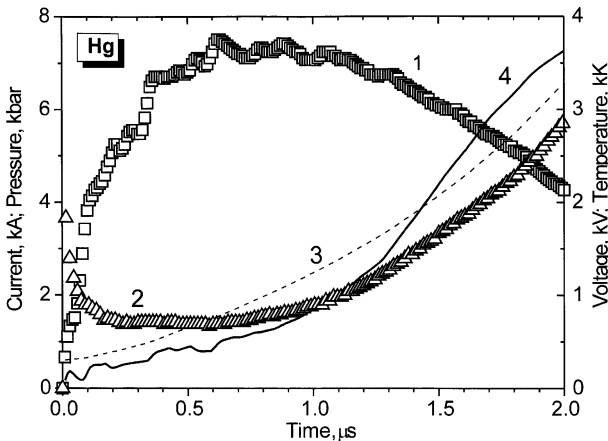


Fig. 2. Temporal dependences of the basic measured (marks) and calculated quantities (lines) for an experiment with Hg sample: current (1); resistive part of the voltage drop (2); temperature (3); pressure (4).

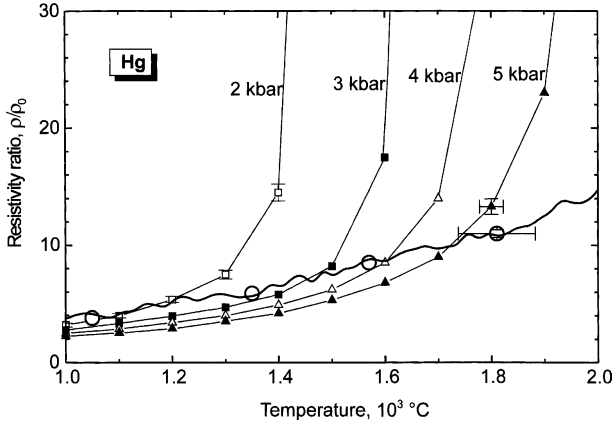


Fig. 3. Relative resistivity versus temperature. Open marks connected by solid lines, isobars [9]; thick line, this work; open circles, the points at which the pressure values 2–5 kbar were achieved in this pulse-heating experiment.

The higher is the pressure, the smoother and flatter is the temperature dependence of the electrical resistivity in the metal–nonmetal transition region (see Fig. 3). This behavior of the electrical resistivity has allowed us to heat the sample to the critical temperature.

4. ELECTRICAL CONDUCTIVITY OF EXPANDED TUNGSTEN

The paths of several heating processes realized in our experiments on tungsten in the p – T plane are presented in Fig. 4. The paths were calculated using the mentioned hydrodynamic model for the prescribed temporal dependences of the Joule heat released and current pulse. Each of the three experiments (2, 3, and 11) is illustrated by two trajectories representing two thin layers in the sample: a surface layer and a layer near the symmetry plane. These two layers correspond to two cells from 50 to 100 cells of the spatial mesh used in these computations. Every layer contains a fixed mass. As follows from Fig. 4, variations of the temperature and pressure across the foil sample did not exceed 10% during the entire heating processes. Such nonuniformities are developed mainly due to the pinch-effect and the effect of inertia in the foil sample when the heating power changes rapidly.

The corresponding dependences of the resistivity versus relative volume (the volume normalized to the specific volume of solid tungsten under standard conditions) are presented in Fig. 5. As can be seen, these

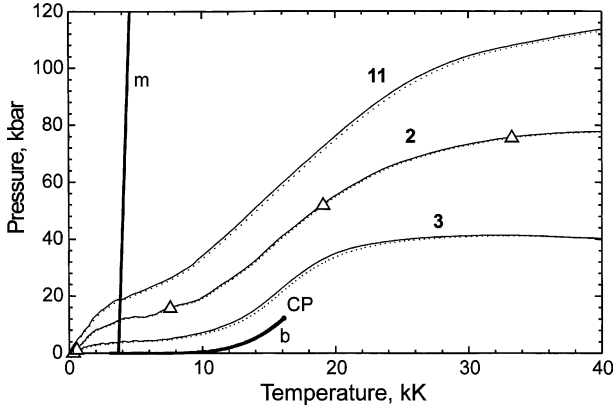


Fig. 4. Evolution of thermodynamic state of a tungsten foil strip placed between glass plates (experiment 3) and sapphire plates (experiments 2 and 11) during the pulse Joule-heating process: (m) melting line; (b) boiling curve; (CP) critical point. The triangles refer to times separated by an interval of 200 ns, starting from the time at which the current is switched on.

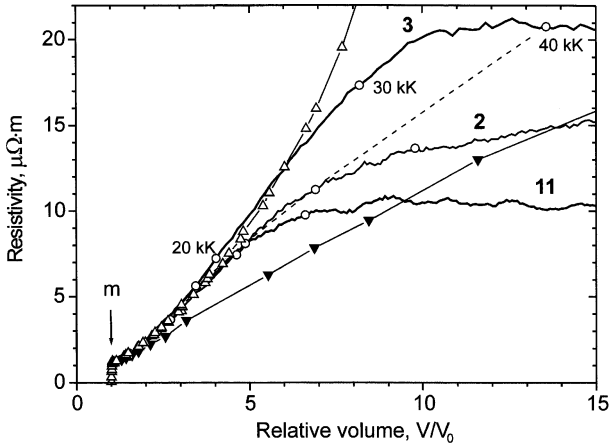


Fig. 5. Resistivity of tungsten versus relative volume: labeled solid lines, this work; open triangles, Ref. 7; closed triangles, Ref. 10. The arrow (m) indicates the melting region. The open circles indicate the points at which the temperature in present experiments achieves the values of 10, 20, 30, 40, and 50 kK. The resistivity along the $T = 40$ kK isotherm derived from this work is shown with the dashed line.

dependences are different for solid, liquid, and gaseous states. The clearly expressed break designated by the arrow (m) indicates the melting region. In the liquid phase, the resistivity is approximately a linear function of the specific volume. Such a form of the dependence is valid up to a relative volume of about 8. Over the range of relative volumes from 9 to 11, the dependence changes its character (experiment 3). For larger relative volumes, the resistivity approaches a nearly constant value. Therefore, we can assume that the resistivity dependence changes its form from metal-like to plasma-like at a density, which is 9 to 11 times lower than the standard solid density. It should be noted that for relative volumes larger than 5, the heating process in experiment 3 was nearly isobaric. Thus, we can emphasize that the resistivity changes its density dependence along an isobar in which it has a pronounced knee in the relative volume range from 9 to 11 (experiment 3). As the pressure increases, the dependence becomes smoother and flatter.

Figure 6 shows the normalized resistance R^* of the sample as a function of the specific Joule heat released for experiments 3, 4, and 11. We present these dependences because both these quantities are measured directly and the dependences can be compared with the data obtained in other studies. We normalize the resistance R by multiplying it by the ratio of the initial cross-sectional area of the foil strip to its length: $R^* = RS_0/l$. For a homogeneously heated sample, the resistance so normalized

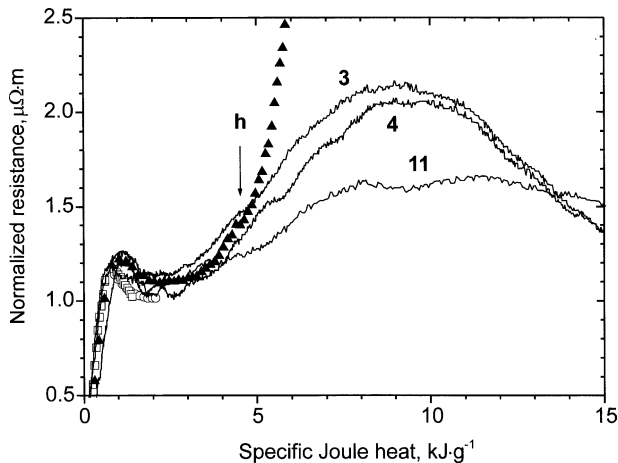


Fig. 6. Normalized resistance versus specific Joule-heat released: this work, lines; closed triangles, [7]; open circles, [13]; open squares, [14]. The arrow indicates the end of the homogeneous heating stage for experiment [7].

is proportional to the ratio of the density to the electrical conductivity. It can be seen from Fig. 6 that our results agree well with the data in Refs. 7 (within the homogeneous heating stage), 13 and 14 within the homogeneous heating stage. In Ref. 7 the electric conductivity was measured at pressures between 10 and 20 kbar and at densities ranging from the standard solid density down to a density four times less. The arrow (h) indicates the end of the homogeneous heating stage for that experiment. The distributions of basic measured quantities across an expanding sample were investigated in Ref. 7 by means of 1D MHD simulations. In Fig. 6 the curve referring to experiment 3 has a pronounced maximum in the range of the specific Joule heat dissipated from 8 to 11 $\text{kJ} \cdot \text{g}^{-1}$. The reproducibility of the data in the region of the maximum is fairly high. To make this evident, we show the data obtained in experiments 3 and 4, which were performed under similar conditions. The two corresponding curves are seen to differ by not more than about 10%. This difference represents the uncertainty of the parameters of our experiments. It follows from the figure that our results differ from the data obtained in Refs. 7, 13, and 14 by the same amount ($< 10\%$).

5. DISCUSSION

At supercritical temperatures and pressures the density dependence of the electrical conductivity of tungsten changes sharply in a narrow density range in which it has a pronounced knee. When the pressure increases from about 30 to 100 kbar, the dependence becomes substantially flatter and smoother. Note that the change of the character of the dependence of the resistivity on the relative volume is directly related to the maximum in the dependence of the normalized resistance on the Joule heat dissipated (see Fig. 6) and, therefore, cannot depend on the accuracy with which the heating dynamics is simulated.

Another interesting feature in the resistivity behavior as a function of density is the following. For a given pressure a characteristic density value exists above which the resistivity merges with a limiting envelope of the resistivity isobars. It can be clearly seen in Fig. 5 that the relative volume at which this takes place depends on pressure. In Ref. 11 the same behavior is discussed for the electrical conductivity of aluminum along isotherms. Examination of the band structure of the metal when its density is lowered has revealed formation of a gap in the electronic density of states near the Fermi energy at a certain density value [11]. In Ref. 11 it is noticed that in the liquid phase at densities larger than the characteristic density at which the gap is formed, the conductivity depends very weakly on the temperature but strongly on density: $\sigma \propto \rho^{7/3}$. The present study

results show that the tungsten conductivity is roughly linearly dependent on density over the density range from the melting point density down to a density 5 to 6 times less. More careful analysis shows that the conductivity dependence can be approximated by $\sigma \propto \rho^n$ only for a density range from the melting point density down to a density four times less ($n \approx 1.2$ – 1.4). At a density about 5 times less than the standard solid density, the dependence changes its curvature.

The data obtained in Ref. 10 differs from those obtained in Ref. 7 and from this work because of a large systematic error in determining the volume and the resistive part of the voltage drop. In the experiments [10], the wires were heated in glass capillaries such that the ratio of the inner diameter of the capillary to the initial wire diameter was eight. The sample volume was determined by recording the luminosity of the expanding plasma column through the thick capillary wall. At the early stage of the process when the wire vaporized, the plasma column was nonuniform which resulted in an additional source of uncertainty.

The theory developed in Ref. 12 yields a resistivity value that is close to that obtained in experiment 3, and an analogous character of the dependence of the resistivity on the specific volume is predicted (in the range $V/V_0 > 19$). The temperature obtained in our calculations for this experiment at a relative volume of 19 is about 46 kK, while the calculations carried out in Ref. 12 refer to the $T = 30$ kK isotherm.

It is of interest to estimate the characteristic density corresponding to the transition of tungsten from a metallic to a dielectric state. According to the predictions in Ref. 15, this transition is continuous and is not a first-order phase transition. The characteristic density is determined from the condition that the fraction of the classically accessible volume for valence electrons of the atoms of which the metal is formed amounts to about 30%. At a low temperature, the corresponding relative volume is approximately equal to five. At a temperature of $T \approx I_1/3$ (where I_1 is the first ionization potential of tungsten), the metal-to-dielectric transition region should completely disappear. For tungsten, this temperature is about 30 kK. Hence, the knee observed in this work (experiment 3) seems to be unrelated to the theoretical predictions of Ref. 15, as the temperature of about 34 kK is achieved near the knee and the corresponding relative volume reaches a value of 10.

6. CONCLUSION

The technique developed can be used to provide homogeneous heating of a tungsten sample and to measure its electrical resistance during a continuous transition from a condensed to a gaseous state. The tungsten

density decreased from the standard solid density to a density 15–20 times less. Using the technique, we have carried out experiments on nearly isobaric heating of tungsten in a gaseous state. We have found that the conductivity-to-density ratio for tungsten in the liquid state remains almost constant at densities ranging from the melting point density down to that approximately 8 to 9 times less. At lower densities, the dependence of the conductivity on the density along the 30 kbar isobar becomes independent of density and approaches a nearly constant value. This change in the character of the dependence manifests itself as a knee in the corresponding experimental curve. As the pressure increases from about 30 to 100 kbar, the density dependence of the conductivity near the knee becomes remarkably flatter and smoother.

We should note one time more, that in this study we did not measure the sample thickness and pressure. These two quantities were derived from 1D MHD simulations of the heating dynamics. Thus, direct measurements of the electrical conductivity along with the complete set of thermodynamic quantities are needed. Now an experimental technique is developed by us to carry out the pressure measurements during the pulse heating process.

REFERENCES

1. Ya. B. Zel'dovich and L. D. Landau, *Zh. Eksp. Teor. Fiz.* **14**:32 (1944).
2. F. J. Benage, W. R. Shanahan, and M. S. Murillo, *Phys. Rev. Lett.* **83**:2953 (1999).
3. A. W. DeSilva and J. D. Katsourous, *Int. J. Thermophys.* **20**:1267 (1999).
4. V. Recoules, P. Renaudin, J. Clerouin, P. Noiret, and G. Zerah, *Phys. Rev. E.* **66**:056412 (2002).
5. V. N. Korobenko and A. D. Rakhel, *Int. J. Thermophys.* **20**:1259 (1999).
6. V. N. Korobenko, A. D. Rakhel, A. I. Savvatimskiy, and V. E. Fortov, *Plasma Physics Reports* **28**:1008 (2002).
7. A. D. Rakhel, A. Kloss, and H. Hess, *Int. J. Thermophys.* **23**:1369 (2002).
8. M. M. Basko, *Teplofiz. Vys. Temp.* **23**:483 (1985).
9. I. K. Kikoin and A. P. Senchenkov, *Fiz. Met. Metalloved.* **24**:843 (1967).
10. S. Saleem, J. Haun, and H.-J. Kunze, *Phys. Rev. E* **64**:056403 (2001).
11. M. P. Desjarlais, J. D. Kress, and L. A. Collins, *Phys. Rev. E* **66**:025401-1 (2002).
12. S. Kuhlbrodt and R. Redmer, *Phys. Rev. E* **62**:7191 (2000).
13. U. Seydel, W. Fucke, and H. Wadle, *Die Bestimmung Thermophysikalischer Daten Flüssiger Hochschmelzender Metalle mit schnellen Pulsaufheizexperimenten* (Verlag Dr. Peter Mannhold, Düsseldorf, 1980).
14. A. Berthault, L. Arles, and J. Matricon, *Int. J. Thermophys.* **7**:167 (1986).
15. A. A. Likal'ter, *Usp. Fiz. Nauk* **162**:119 (1992) [*Sov. Phys. Usp.* **35**:591 (1992)].